Development and comparison of chromatographic methods for the analysis of long chain diols and alkenones in biological materials and sediment

Marijke W. de Bar,*[,†] Ellen C. Hopmans,[†] Monique Verweij,[†] Denise J. C. Dorhout,[†] Jaap S. Sinninghe Damsté[†,‡] and Stefan Schouten[†,‡]

[†] NIOZ Royal Netherlands Institute for Sea Research, Department of Marine Microbiology and Biogeochemistry, and Utrecht University, P.O. Box 59, 1790 AB Den Burg, Texel, the Netherlands

[‡] Utrecht University, Faculty of Geosciences, P.O. Box 80115, 3508 TC Utrecht, the Netherlands

* Corresponding author. Tel.: + 31 (0)222 369 569. E-mail: Marijke.de.Bar@nioz.nl

To be submitted to: *Journal of chromatography A*

Abstract

We have compared and assessed the suitability of several chromatographic methods for the analysis of long chain alkenones and long chain diols and the associated paleotemperature proxies ($U^{K'}_{37}$ and LDI). We evaluated the traditional methods for the analysis of the $U^{K'}_{37}$ and the LDI, gas chromatography (GC) - flame ionization detection (FID) and GC mass spectrometry (MS) using selected ion monitoring (SIM), respectively, and developed a new method using GC-MS/MS in multiple reaction monitoring mode (MRM) for the analysis of long chain diols as well as a method for automatic silylation of diols using a robot autosampler.

Finally, we evaluated liquid chromatography (LC) methods to simultaneously measure the $U^{K'}_{37}$ and the LDI, using ultra high performance LC (UHPLC) with low (nominal mass) resolution MS in SIM mode, and UHPLC with high resolution MS (HRMS). Detection and quantification limits and reproducibility were assessed by means of serial dilutions of culture extracts.

Automated silylation by robot autosampler showed similar reproducibility as off-line silylation while substantially decreasing sample preparation time. The novel MRM method had a slightly lower limit of quantification (LOQ; i.e. 0.3 pg C_{28} 1,13-diol injected on-column) than the traditional method (0.5 pg) and improved reproducibility while allowing more unambiguous identification of LCDs in complex matrices. For diols, UHPLC-MS using SIM had the highest LOQ (i.e. 15 pg) and a comparable reproducibility as GC-MS. UHPLC-HRMS had a LOQ of ca. 1.5 pg, and an improved reproducibility for diol analysis. For alkenone analysis, both UHPLC-HRMS and UHPLC-MS using SIM were 2-3 orders of magnitude more sensitive (LOQ ca. 20 and 2 pg $C_{37:2}$ alkenone injected on-column, respectively) than GC-FID (LOD ca. 3 ng), with a similar reproducibility of the $U^{K'}_{37}$ index. Hence, UHPLC-HRMS allows simultaneous analysis of the $U^{K'}_{37}$ and LDI at an increased sensitivity. In addition, it allows simultaneous measurement of TEX_{86}, a temperature proxy based on the isoprenoid glycerol dialkyl glycerol tetraethers. This reduces the preparation time by excluding the need of derivatization and separation of the ketone (containing the long chain alkenones) and polar fractions (containing the long chain diols and GDGTs). However, synthetic standards are required to fully assess the accuracy of the new methods for determination of the LDI and $U^{K'}_{37}$.

Keywords: LDI; $U^{K'}_{37}$; diols; alkenones; GC-MS MRM; UHPLC-MS

1. Introduction

Future climate conditions can be better assessed if we have knowledge of past climate and oceanic responses to past climate perturbations. The reconstruction of past temperatures is one of the main goals for paleoceanographers as temperature is an important boundary condition for identifying the processes and mechanisms responsible for past climate changes. Two organic proxies, the TEX_{86} based on glycerol dialkyl glycerol tetraethers (GDGTs) [1] and $U^{K'}_{37}$, based on long chain alkenones (LCAs) [2] (Fig. 1) have been developed, and are now commonly applied in reconstructing past sea water temperatures. Recently, a new index has been proposed, the Long chain Diol Index (LDI) [3], based on the distribution of specific long chain diols (LCDs) occurring in marine sediments (Fig. 1) [4,5], likely derived from eustigmatophyte algae. Thus, it is now possible to use a multiproxy approach using three independent organic proxies to constrain past seawater temperatures. This is often preferred as every proxy has its limitations, and therefore the comparison between different proxies can shed more light on these shortcomings, and result in better constrained temperature reconstructions.

The traditional method for the analysis of LCAs is gas chromatography-flame ionization detection (GC-FID) [6]. Although this method separates and quantifies LCAs satisfactorily, there are disadvantages such as the co-elution of long chain alkenoates and adsorption effects [7,8], and studies have therefore focused on e.g. sample clean up [9], different GC stationary phases [10], multidimensional GC [11] and new detection methods such as GC-chemical ionization mass spectrometry (GC-CI-MS) [12,13], GC-electron ionization MS (GC-EI-MS) in selected ion monitoring (SIM) mode [14], and GC time-of-flight MS (GC-TOF-MS) [15]. Two studies have evaluated the possibility to analyze LCAs by means of liquid chromatography (LC)-MS. Schwab et al. [16] presented a semi-preparative normal phase high pressure LC-MS (NP-HPLC-MS) protocol for purifying C_{37} and C_{38} LCAs and Becker et al. [17] proposed a

74 method for the quantitation of the C_{37} and C_{38} LCAs using LC-qTOF- high resolution MS (LC-
75 qTOF-HRMS). Despite all these developments, LCA analysis by means of GC-FID is still the
76 most preferred method as the instrumentation is relatively cheap and easy to use, and the
77 chromatographical separation and the sensitivity is generally sufficient.
78 GDGTs, which are used for the TEX_{86} index, are analyzed by normal phase high performance
79 liquid chromatography coupled to atmospheric pressure chemical ionization mass spectrometry
80 (NP-UHPLC-APCI-MS), and were initially quantified in full scan (*m/z* 950-1450) by peak
81 integration of the $[M+H]^+$ and $[M+H]^+$+1 (protonated molecule and isotope peak) [1,18,19].
82 Presently, GDGTs are analyzed by SIM of the protonated molecules $[M+H]^+$ [20]. In 2013, a
83 new HPLC protocol using reversed phase (RP) combined with electrospray ionization (ESI)
84 MS was proposed for the analysis of GDGTs, enabling comprehensive analysis of intact polar
85 lipid (IPL) and core GDGTs [21]. Becker et al. [22] proposed a new method with improved
86 chromatography for the isoprenoid core GDGTs, using two UHPLC BEH HILIC amide
87 columns in tandem. Recently, improved NP separation of core GDGTs was achieved using two
88 UHPLC silica columns in series, in combination with the APCI-MS detection method [23].
89 Finally, LCDs are commonly analyzed by GC-MS of their silylated derivatives and quantified
90 using SIM [3]. GC separates the diols based on chain lengths but not on mid-chain alcohol
91 position. MS analysis, however, allows identification of the specific mid-chain isomers based
92 on fragment ions formed by cleavage adjacent to the OTMSi groups (silylated hydroxyl groups)
93 and quantification is achieved by SIM analysis of these specific fragment ions [3,4]. The
94 contributions of these selected ion fragments to the total ion counts for the different LCDs is
95 taken into account and corrected for. Unfortunately, LCD analysis requires substantial work up
96 time because of derivatization, and injection of silylated polar fractions of sediment extracts
97 often results in major build-up of column contamination, limiting sample throughput. Recently,
98 it was shown that diols can also be analyzed by UHPLC-HRMS in which diols are separated

on the basis of their mid-chain alcohol position rather than on chain length [17]. Analysis of LCDs by LC-MS offers several advantages, i.e. no derivatization is needed, therefore contamination by silylation reagents is avoided, and sample preparation is less time consuming. Another advantage of this approach is that other lipids used as proxies for past climate conditions can be measured simultaneously, i.e. GDGTs for the TEX_{86} temperature proxy, and LCAs used in the $U^{K'}_{37}$ index, substantially improving sample throughput. However, an UHPLC-HRMS is relatively expensive and therefore not readily available in paleoclimate geochemical labs. Furthermore, it is not clear how well the sensitivity and accuracy of LCD and LCA analysis on an UHPLC-HRMS compares with that of the more traditional GC-MS and GC-FID, respectively.

Here we evaluated different analytical methods for the identification and quantification of lipids for paleotemperature assessment (see Table 1 for overview). The ideal method would be one that allows the simultaneous analysis of multiple proxies, i.e. the TEX_{86}, $U^{K'}_{37}$ and LDI, i.e. UHPLC-HRMS [17]. However, since most paleoclimate geochemical labs have less advanced MS equipment, we have evaluated this approach using both low (nominal mass) resolution MS and HRMS. In addition, we developed a novel method for diol analysis using GC-MS/MS in multiple reaction monitoring (MRM) mode and compare this with the UHPLC-MS and traditional GC-SIM methods. Furthermore, we developed an automated silylation procedure using a robot autosampler to minimize preparation time for GC-analyses.

2. Experimental section

2.1 Samples and extraction

2.1.1 Long chain diols

LCDs were extracted from *Nannochloropsis oculata* biomass (Reed Mariculture, Inc., San Jose, USA). After freeze-drying, the biomass (46.9 g dry weight) was saponified (following de Leeuw et al. [24] and Rodrigo-Gámiz et al. [25]) by refluxing for 1 h with 1 N potassium hydroxide (KOH) in methanol (MeOH) (96%). Subsequently, 2 N hydrochloric acid (HCl)/MeOH (1:1, vol./vol.) was added to obtain a pH of 3. The extract was then transferred to a separatory funnel filled with bidistilled water. The residue was washed with MeOH/H_2O (1:1, vol./vol.), MeOH (two times) and dichloromethane (DCM) (three times), and these solvents were pipetted in the separatory funnel. The DCM layer was collected in a round-bottom flask. The solvent was removed by rotary evaporation. Subsequently, water was removed from the total lipid extract (TLE) over anhydrous Na_2SO_4 using a Pasteur pipette, and the TLE was dried down under N_2. The TLEs were separated by column chromatography, for which activated (for 2 h at 150 °C) Al_2O_3 was used as stationary phase, using 3 column volumes DCM and DCM/MeOH (95:5, vol./vol.) as eluents to yield the apolar and polar fractions, respectively. Prior to GC-MS analysis, aliquots of the polar fraction were silylated by means of addition of BSTFA (*N,O*-bis(trimethylsilyl)trifluoroacetamide) and pyridine, and heating of the sample at 60 °C for 20 min. For GC-MS/MS analysis the polar fraction was silylated by a robotic autosampler (see below). In case of LC-MS analysis, an aliquot of the polar fraction was re-dissolved in hexane/isopropanol (99:1, vol./vol.), and filtered over a 0.45 µm PTFE filter. For quantification purposes we added a C_{22} 7,16-diol internal standard (31.0 µg) to the polar fractions (MolPort SIA, Latvia).

A selected set of sediment extracts and one river suspended particulate matter (SPM) sample with a range of LDI values were analyzed on GC-MS/MS in MRM mode and GC-MS in SIM mode. These samples derive from the Iberian Atlantic margin and the Tagus river, collected during the PACEMAKER 64PE332 cruise with the R/V Pelagia in 2011 [26,27]. Furthermore, to evaluate the simultaneous analysis of LCDs, LCAs and isoprenoid GDGTs by means of

147 UHPLC-HRMS, we also analyzed a lipid extract from a sediment sample derived from
148 sediment core 434G (252.5 cm) (Alboran Sea, latitude: 36'12.313N, longitude: 4'18.735W;
149 depth: 1108 mbsl, sample interval: 231.25 – 232.75 cm) recovered during the TTR-17 cruise
150 with the R/V Professor Logachev [28]. All samples were extracted by means of accelerated
151 solvent extraction (ASE) and polar fractions were obtained by column chromatography as
152 described previously by Rodrigo-Gámiz et al. [28] for the Alboran Sea and Zell et al. [26,27]
153 for the Iberian Atlantic margin and Tagus river.

154

155 The LDI was calculated according to Rampen et al. [3]:

156 $$\mathrm{LDI} = \frac{F_{\mathrm{C_{30}1,15-diol}}}{F_{\mathrm{C_{28}1,13-diol}} + F_{\mathrm{C_{30}1,13-diol}} + F_{\mathrm{C_{30}1,15-diol}}} \quad [1]$$

157 where F_x indicates the fractional abundance of the diol. Sea surface temperature (SST) is
158 calculated from the LDI index based on the following relation:

159 $$\mathrm{LDI} = 0.033 \times \mathrm{SST} + 0.095 \qquad (R^2 = 0.969;\ n = 162) \quad [2]$$

160

161 *2.1.2 Long chain alkenones*

162 LCAs were extracted from freeze-dried *Emiliani huxleyi* biomass obtained by collecting
163 washed out cells from a continuous culture. The biomass was extracted by sonication using
164 DCM/MeOH (2:1, vol./vol.) according to Chivall et al. [29]. The TLE was separated over
165 activated Al_2O_3, using 4 column volumes of *n*-hexane/DCM (9:1, vol./vol.), *n*-hexane/DCM
166 (1:1, vol./vol.) and 3 column volumes of DCM/MeOH (1:1, vol./vol.) as eluents to yield the
167 apolar, ketone and polar fractions, respectively. The fraction was dissolved in ethyl acetate prior
168 to analysis on GC-FID, and in hexane/isopropanol (99:1, vol./vol.), and filtered over a 0.45 µm
169 PTFE filter prior to injection on LC-MS. For quantification purposes, a 10-nonadecanone ($C_{19:0}$
170 ketone; 300.8 µg; Aldrich Chemical Company, Inc., USA) internal standard was added to the

171 extract.

172

173 The $U^{K'}_{37}$ index as described by Prahl and Wakeham [30] was calculated:

174 $$U_{37}^{K'} = \frac{[C_{37:2}\ \text{alkenone}]}{[C_{37:2}\ \text{alkenone}] + [C_{37:3}\ \text{alkenone}]} \quad [3]$$

175 The $U^{K'}_{37}$ values were converted to SST using the following equation [31]:

176 $$U_{37}^{K'} = 0.033 \times \text{SST} + 0.044 \qquad (R^2 = 0.958;\ n = 370) \quad [4]$$

177

178 *2.2 Instrumentation*

179 *2.2.1 GC-FID*

180 GC-FID analysis of LCAs was performed using an Agilent 6890N GC with FID and mounted
181 with a 50 m fused silica column (diameter 0.32 mm) coated with CP Sil-5 (thickness 0.12 µm)
182 (e.g. Rodrigo-Gámiz et al [25]). Helium was used as carrier gas. The oven program started at
183 70 °C upon injection, and T was subsequently increased by 20 °C per minute to 200 °C, and
184 finally by 3 °C per minute until 320 °C. The final temperature of 320 °C was held for 30 min.
185 A constant pressure of 100 kPa was maintained and samples were injected on-column. The
186 alkenone fraction of the *E. huxleyi* extract, containing LCAs, was serially diluted to assess the
187 limit of detection and quantitation (LOD and LOQ), and these dilutions were measured in
188 duplicate.

189

190 *2.2.2 GC-MS*

191 GC-MS analysis of LCDs present in silylated polar fractions was carried out on an Agilent
192 7890B gas chromatograph coupled to a Agilent 5977A mass spectrometer. Samples were
193 dissolved in ethyl acetate and injected at 70 °C. The oven temperature was programmed to 130
194 °C by 20 °C/min, and subsequently to 320 °C by 4 °C/min; this temperature was held for 25

min. The GC was equipped with an on-column injector and fused silica column (25 m x 0.32 mm) coated with CP Sil-5 (film thickness 0.12 µm). Helium was used as carrier gas at a constant flow of 2 mL/min. The mass spectrometer operated with an ionization energy of 70 eV and a cycle time of 1.9 s. The temperature of the ion source was 250 °C, and of the interface 320 °C. The injection volume was 1 µL. The LCDs were identified by means of the characteristic fragmentation spectra in full scan mode, using a *m/z* range of 50-800 [4]. Quantification of the different diol isomers was achieved by selective ion monitoring (SIM) mode scanning of the characteristic fragment ions, i.e. *m/z* 299, 313, 327, 341 and 355, with a gain factor of 3 and a dwell time of 100 ms. The runtime was 75.5 min. Serial dilutions of polar fraction of the *N. oculata* extract were analyzed in full scan and SIM mode in triplicate.

2.2.3 GC-MS/MS

GC-MS/MS analysis of LCDs was performed on an Agilent 7890B GC system interfaced to a 7000 C / Triple Quadrupole MS, in multiple reaction monitoring (MRM) mode. An Agilent 7693 robotic autosampler was used to silylate the polar fractions. For this purpose, a small aliquot of the polar fraction was transferred into an autosampler vial with a 250 µL insert and the solvent was evaporated using nitrogen. Firstly, 10 µL pyridine was added, after which the sample was shaken at 2500 rpm for 5 × 5 sec. Subsequently, 10 µL BSTFA was added, and the sample was shaken again at 2500 rpm for 5 × 5 sec. The sample was then heated at 60 °C for 20 min, after which the sample was kept at room temperature for 10 min. Next, 100 µL ethyl acetate was added and the sample was shaken at 3000 rpm for 5 × 10 sec, left for 30 sec, and again shaken at 3000 rpm for 5 × 10 sec. Subsequently, 0.5 µL out of 120 µL was injected on-column. Oven program, column, carrier gas and MS settings were the same as for GC-MS described above, apart from the interface temperature which was 330 °C and a runtime of 60.5 min (kept for solely 10 min at 320 °C). Serial dilutions of the *N. oculata* fractions were analyzed

in SIM and MRM mode in triplicate. The environmental samples deriving from the Iberian margin, to assess the relationship between SIM and MRM derived LDI values, were analyzed once.

2.2.4 NP-UHPLC-APCI-MS

NP-UHPLC-APCI-MS analysis of LCDs and LCAs was performed using an Agilent 1260 UHPLC, equipped with automatic injector, coupled to a 6130 Agilent single quadrupole MSD with HP Chemstation software. The method has been previously been described by Hopmans et al. [23] for the analysis of GDGTs. Briefly, separation of LCDs and LCAs was achieved using 2 silica BEH HILIC columns in series (150 mm x 2.1 mm; 1.7 µm; Waters Acquity), kept at 25 °C. The compounds were eluted isocratically with 82% A and 18% B for 25 min, followed by a gradient to 35% B in 25 min and 100% B, kept for 20 min, where A = hexane and B = hexane/isopropanol (90:10, vol./vol.). Flow rate was kept constant at 0.2 mL/min. Maximum pressure during analysis was 400 bar. The total run time was 102 min followed by 20 min re-equilibration, for LCDs. For LCAs the total run time was shortened to 26 min, i.e. using solely isocratic elution, however, in case of multi-proxy analysis, a total run time of 102 minutes is needed. Conditions for the APCI-MS were as follows: nebulizer pressure 60 psi, vaporizer temperature 400 °C, drying gas (N_2) flow 6 L/min and temperature 200 °C, capillary voltage -3kV, corona 5 µA. Initially detection of diols was achieved by monitoring *m/z* 375 to 525. In general, a 10 µL injection volume was used. For determination of LOD and LOQ, serial dilutions of both the *N. oculata* and *E. huxleyi* fractions were analyzed in triplicate in SIM mode. For the LCDs the $[M+H]^+$-18 ions with *m/z* 409 (C_{28}), 437 (C_{30}), 451 (C_{31}), 465 (C_{32}), 493 (C_{34}) and 521 (C_{36}) were integrated, whereas for the $C_{37:2}$ and $C_{37:3}$ LCAs the $[M+H]^+$ protonated molecule traces were integrated, i.e. *m/z* 531 and 529, respectively.

245 *2.2.5 UHPLC-HRMS*

246 UHPLC- high resolution MS (HRMS) was performed using an Ultimate 3000 RS UHPLC
247 equipped with thermostatted auto-injector and column compartment coupled to a Q Exactive
248 (Quadrupole Orbitrap hybrid MS) MS equipped with ion max source with APCI probe (Thermo
249 Fisher Scientific, USA). The Q Exactive was calibrated within a mass accuracy range of 1 ppm
250 using the Thermo Scientific Pierce LTQ Velos ESI Positive Ion Calibration Solution
251 (containing a mixture of caffeine, MRFA, Ultramark 1621, and N-butylamine in an
252 acetonitrilemethanol-acetic solution). The positive-ion APCI settings were as follows: capillary
253 temperature 275°C, sheath gas (N_2) 50 arbitrary units (AU); auxiliary gas (N_2) 5 AU, corona
254 current 4.5 µA, APCI heater temperature 275 °C and S-lens 50 V. Separation was achieved
255 using the identical chromatographic conditions as described above for the UHPLC-single
256 quadrupole MS measurements.
257 Detection of LCDs, LCAs and GDGTs was achieved in positive ion mode by scanning *m/z* 400-
258 1450 with a resolution of 17,500 ppm mimicking the resolution of a typical TOF MS.
259 Quantifications were done by integrating mass chromatograms (smoothed with Gaussian factor
260 7) within 20 ppm mass accuracy of the protonated molecules (LCAs and GDGTs) or the
261 protonated molecules after loss of water ($[M+H]^+$-H_2O) in case of LCDs. Serial dilutions of
262 both the *N. oculata* and *E. huxleyi* fractions were analyzed in triplicate.

263 To determine the elution order of the LCD isomers on the UHPLC-MS, LCD isomers of the
264 *Nannochloropsis oculata* culture were isolated by separation on the Agilent 1260 UHPLC with
265 identical chromatography (2 x BEH HILIC Si [23]) as described above, and subsequent
266 collection of half minute intervals by an ISCO Foxy Jr. fraction collector. The solvent in the
267 collection vials within the diol time window (15 – 30 min) were evaporated under N_2, the
268 fractions were silylated and analyzed by GC-MS.

269

3. Results and discussion

3.1 Development and evaluation of different methods for the analysis of LCDs

The traditional method for quantification of LCDs, as well as computation of the LDI, is single quadrupole GC-MS using SIM, as introduced by Rampen et al. [3]. We developed a new method, using triple quadrupole GC-MS/MS using MRM to improve selectivity compared to SIM detection. Moreover, we developed a method for the automatic silylation of polar fractions using a robot autosampler to increase sample throughput. Additionally, a multi-proxy analytical method using UHPLC-HRMS modified from Becker et al. [17] was evaluated in terms of sensitivity. Besides UHPLC-HRMS, we also analyzed LCDs using UHPLC- single quadrupole MS in SIM mode (see Table 1 for overview of methods). For both approaches the UHPLC chromatographic protocol according to Hopmans et al. [23] (i.e., 2 × BEH HILIC Si) was used. Below, we will first discuss the development of automated silylation combined with MRM analysis using triple quadrupole GC-MS/MS, followed by the analysis of diols on UHPLC-HRMS and UHPLC-MS.

3.1.1 Automated silylation

Traditionally, polar fractions are silylated manually in the laboratory prior to injection by addition of two silylation reagents (pyridine and BSTFA) and heating for >20 min, followed by the addition of the injection solvent (mostly ethyl acetate). Here, a robot autosampler was used for automatic silylation of the polar fractions, meaning that during a sequence of analyses each fraction is derivatised during the analysis of the prior sample. This is a major advantage in case of large sample sets, saving substantial work-up time, and ensuring that compounds are derivatised freshly at the time of analysis. The most important parameter to optimize was mixing efficiency, i.e. the combination of mixing time and mixing speed (rpm), to ensure

294 complete mixing of the derivatizing reagents pyridine and BSTFA with the injection solvent
295 ethyl acetate in the 205 µL insert vials. For this purpose, several aliquots of the *N. oculata*
296 extract were automatically silylated and after addition of solvent, shaken at different mixing
297 speeds for different durations. Comparisons of the resulting diol peak areas showed that the
298 largest diol peak areas were obtained with a mixing time and speed of 5 × 10 s at 3000 rpm,
299 which was done twice with a 30 s pause in between. Subsequently, we compared the overall
300 yield of diol derivatization of automatic silylation with manual silylation by derivatization and
301 analysis of the C_{22} 7,16-diol standard (in quintuplicate). The difference in peak area between
302 manual silylation and robot silylation (ca. $1.1e^8$ and $9.6e^7$, respectively) is statistically not
303 significant (two-tailed t-test *p*-value = 0.10) and the reproducibility of both derivatization
304 methods is highly comparable: 9.4% and 9.7%. This confirms the robustness of the automated
305 silylation method.

306

307 *3.1.2 MRM analysis using triple quadrupole GC-MS/MS*

308 We developed methodology for the detection of LCDs using MRM. For a reliable identification
309 we used two MRM transitions: one to quantify the diol (quantifier) and another to confirm the
310 identity of the diol (qualifier). For the first MRM transition (quantification), we selected the
311 ions *m/z* 299 (e.g., C_{28} 1,14), 313 (e.g., C_{28} 1,13; C_{30} 1,15) , 327 (e.g., C_{30} 1,14) and 341 (e.g.,
312 C_{30} 1,13) as parent ions (Table 2), as these are the most dominant ions produced during electron
313 ionization, and commonly used in GC-MS SIM analysis of diols [3,4]. We examined their MS^2
314 product spectra after collision induced dissociation with helium and nitrogen. The resulting
315 MS^2 fragmentation spectra reveal *m/z* 73 as the dominant fragment as well as *m/z* 103 as
316 characteristic product ions for all parent ions, representing the $[TMSi]^+$ and $[CH_2OTMSi]^+$
317 groups, respectively (see Fig. 2b for *m/z* 313 as parent ion for the C_{30} 1,15-diol). Although *m/z*
318 73 is much more abundant than *m/z* 103 ion, the latter is more characteristic for LCDs as it is

mostly derived from the midchain TMSi group and consequently this ion was selected in MS^2 as the product ion for all LCD parent ions. The collision energy was optimized for maximum yield of the *m/z* 103 product ion for each individual LCD (Table 2). The parent ions selected in MS^1 for the second transition (qualification), are the more minor fragments generated from the opposite α-cleavage of the mid-chain silylated alcohol group (see Fig. 2), corresponding to *m/z* 359, 373 and 387 for the 1,13, 1,14 and 1,15 diols [4]. In the MS^2 spectrum of these qualifier ions, one of the major fragments is *m/z* 109 (C_8H_{13}), which was selected as the product ion. Also for this product ion, the collision energy for the production of this fragment was optimized for maximum yield (Table 2).

3.1.3 NP-UHPLC-(HR)MS

Becker et al. [17] showed the possibility of a multi-proxy analysis using UHPLC-MS. We tested this approach using normal phase chromatography of Hopmans et al. [23] as it has been shown that it results in an improved chromatographic resolution for GDGTs. First we performed a full scan analysis (using single quad MS) to verify the dominant formation of the $[M+H]^+$-18.0 Da (loss of water) for the LCDs over the $[M+H]^+$ after APCI as described by Becker et al. [17]. The LCDs eluted in a time window of 16 to 24 min (Fig. 3b). The elution order of the various diols was confirmed by analyzing collected 30 s effluent fractions with GC-MS. This showed that the normal phase UHPLC method of Hopmans et al. [23] (2 silica BEH HILIC columns) also results in the separation of LCDs based on the mid-chain position of the hydroxyl group, as observed earlier by Becker et al. [17] (2 amide BEH HILIC columns).

3.2 Comparison of LCD analysis methods

We compared five different methods for the quantitation of LCDs: single quadrupole GC-MS using SIM, triple quadrupole GC-MS/MS in SIM mode using the 3rd quadrupole only, triple

quadrupole GC-MS/MS using MRM, single quadrupole UHPLC-MS using SIM and Orbitrap UHPLC-HRMS set at a resolution of 17,500 (Table 1). The latter resolution is somewhat lower compared to the 27,000 used by Becker et al. [17] but in the range of typical LC-TOF-MS equipment which are less expensive.

3.2.1 LOD and LOQ

We determined the limit of detection (LOD) (signal-to-noise ratio (S/N) of > 2) of the C_{28} 1,13-diol (as this was the lowest abundant LCD in the culture extract) and the limit of quantitation (LOQ) of the LDI by repeated analysis of serial dilutions of an extract of *N. oculata* biomass as there are currently no synthetic standards of naturally occurring C_{28}-C_{32} LCDs available. The dominant LCDs present in the *N. oculata* extract are the C_{28} 1,13-, C_{30} 1,13- and 1,15-, C_{31} 1,15-, C_{32} 1,15-, C_{34} 1,17- and the C_{36} 1,19-diol. In order to determine the abundance of the C_{28} 1,13-diol in the extract we added a known amount of a C_{22} 7,16-diol synthetic standard and analyzed the extract by GC-MS in SIM mode. The C_{28} 1,13-diol and C_{22} 7,16-diol were quantified by integrating mass traces *m/z* 313 and *m/z* 187, respectively. A correction of 27% and 16% for the C_{22} 7,16- and C_{28} 1,13-diol, respectively, was applied for the contributions of these fragment ions to the total ion counts. The LOQ is defined as the amount of the C_{28} 1,13-diol at which the LDI index significantly deviated from the average LDI determined at higher concentrations.

In Fig. 4 the LDI values versus different amounts of C_{28} 1,13-diol injected are shown for the different methods. The lowest LOD was obtained by MRM analysis, corresponding to ca. 0.05 pg C_{28} 1,13-diol injected on-column. However, the LDI value at this LOD is significantly different from the values at higher concentrations (two-tailed t-test *p*-value << 0.05) and therefore we define the LOQ for the LDI as ca. 0.3 pg LCD injected on-column based on the first higher concentration injected. The LOD and LOQ were slightly higher for SIM analysis

on both the single quadrupole MS or the triple quad MS with LODs and LOQs of ca. 0.5 pg C_{28} 1,13-diol injected on-column (Fig. 4). The slightly improved LOD and LOQ of the MRM method compared to a SIM approach is probably due to the elimination of non-targeted compounds and background. This is further demonstrated by the analysis of an environmental sample (Tagus River SPM, Portuguese margin [27,32]) using MRM (Fig. 5) revealing considerably improved signal-to-noise ratios compared to SIM. The LOD obtained for Orbitrap UHPLC-HRMS is higher than that of both MRM and SIM analysis using GC-MS, being around ca. 1.5 pg C_{28} 1,13-diol injected on-column (Fig. 4). Since at this concentration the LDI is significantly different from the LDI at higher concentrations (two-tailed t-test p-value < 0.05), the LOQ is defined as ca. 3 pg C_{28} 1,13-diol injected on-column. This LOQ is in the same order of magnitude as reported by Becker et al. [17] for LC-qToF-MS ("<10 pg"). However, we observed substantial variations in LOD/LOQ for our triplicate measurements due to variability in background signals, probably due to differences in solvent batches used as mobile phase. Single quadrupole UHPLC-MS reveals a LOD, as well as LOQ, of around ca. 15 pg C_{28} 1,13-diol, i.e. a lower sensitivity compared to GC-MS and UHPLC-HRMS.

3.2.2 Reproducibility and linearity

The reproducibility of the LDI index was, as observed for the sensitivity, better for GC-MS MRM (±0.0030, n = 24 when solely data above LOQ is considered; reproducibility visualized as error bars in Fig. 4), compared to reproducibility's of ±0.0052 (n = 21) and ±0.0049 (n = 21) we obtained on the single and triple quadrupole GC-MS systems in SIM mode, respectively. The reproducibility of the LDI on UHPLC-HRMS was ±0.0027 (n = 30 above LOQ), similar to the MRM method on GC-MS and better than the single and triple quad GC-MS(/MS) in SIM mode. The reproducibility on UHPLC-MS was ±0.0053 (n = 30). The responses (peak area versus amount of C_{28} 1,13-diol (pmol) injected on-column) were linear for all methods over the

394 measured decades (Table 3).

395

396 *3.2.3 Comparison of LDI values*

397 We compared the LDI values of the *N. oculata* extract obtained by the five different analysis
398 methods and only considered data above the LOQ (Fig. 6). For the commonly used SIM
399 analysis the LDI was 0.276±0.0052 and 0.287±0.0049 for the single and triple quadrupole MS,
400 respectively, which is statistically different. In fact, all LDI values obtained by the different
401 methods are significantly different from each other (two-tailed t-test *p*-value << 0.05 for all
402 methods). The average LDI values for UHPLC-MS and UHPLC-HRMS are quite similar with
403 values of 0.216±0.0053 and 0.224±0.0027, respectively. Hence, whereas the difference in LDI
404 between the single and triple quadrupole GC-MS was solely 0.011, and the difference between
405 UHPLC low (nominal mass) resolution MS and HRMS 0.007, the average difference between
406 GC-MS and UHPLC is the largest at 0.062. Becker et al. [17] analyzed a sample set with LDI
407 values varying between 0.58 and 0.98 on GC-MS, and showed that the linear relationship was
408 close to the 1:1 line, but the mean Δ_{LDI} between GC and LC was ± 0.03. Hence, in spite of the
409 almost 1:1 relationship, there is a clear difference in absolute LDI values derived from UHPLC
410 and GC-MS. Accordingly, standards are required to monitor the relative responses of the LDI
411 LCDs on LC-MS. The MRM method reveals an average LDI value of 0.36 for the *N. oculata*
412 extract, i.e., significantly higher than the LDI values in SIM method (Fig. 6). For further
413 comparison, we measured the LDI in MRM and SIM in a number of environmental samples
414 from the Iberian Atlantic margin [26,27,32]. The resulting LDI values show a strong linear
415 correlation (Fig. 7; R^2 = 0.99; slope = 0.84). However, note that this relation is not 1:1, with
416 LDI values derived from MRM being generally higher than those from SIM for lower LDI
417 values. This is not unexpected, as the relative peak areas of the LCDs are different in the MRM
418 compared to SIM due to the different fragment yields of *m/z* 103 from the target ions (*m/z* 299,

313, 327 and 341). Hence, because of these different responses as compared to SIM, authentic LCDs standards will be required to assess the response of the individual LCDs, posing a severe limitation on this MRM method.

3.3 Comparison of methods for LCA analysis

Though many studies have focused on different methods for the analysis of LCAs, the most applied method is still GC-FID due to the relative simplicity of the method, the sufficient sensitivity and chromatographic separation and the consistency in $U^{K'}_{37}$ results between different laboratories [33]. However, the recently proposed UHPLC-HRMS approach of Becker et al. [17] offers the key advantage of the potential analysis of LCAs simultaneously with other biomarkers used in paleothermometry (i.e. GDGTs and LCDs). Similar to Becker et al. [17], the NP chromatography of Hopmans et al. [23] allows the computation of the LDI. However, the applicability of this UHPLC method for the determination of the $U^{K'}_{37}$ index needs to be investigated. We therefore also determined LOQ and LOD for LCAs, using the identical chromatography as for the LCDs (2 x BEH HILIC Si [23]), combined with HRMS and low (nominal mass) resolution MS using SIM, and compare this with the traditional GC-FID method.

3.3.1 NP-UHPLC-(HR)MS

We analyzed the ketone fraction of an extract of the coccolithophorid alga *E. huxleyi*. This fraction mainly contains the $C_{37:3}$, $C_{37:2}$, $C_{38:3}$, $C_{38:2}$, $C_{39:3}$ and $C_{39:2}$ LCAs, $C_{36:2}$ fatty acid ethyl ester and $C_{36:3}$ and $C_{36:2}$ fatty acid methyl esters. The dominant ions for the $C_{37:2}$ and $C_{37:3}$ LCAs formed with APCI ionization are the $[M+H]^+$ protonated molecules [17]. Similar to the separation of the LCDs, the application of the NP-UHPLC [23] method results in LCA

443 separation based on the position of the carbonyl group, and not the chain length (as obtained
444 using GC); i.e., the ethyl and methyl LCAs are separated, but the $C_{37:2}$ and $C_{37:3}$ methyl LCAs
445 (used in the $U^{K'}_{37}$) co-elute with a retention time of 4-5 min (Fig. 3a). In contrast, the
446 chromatographic protocol of Becker et al. [22] results in the chromatographic separation of the
447 C_{37} LCAs. The C_{38} and C_{39} ethyl ketones, as well as the di- and tri-unsaturated C_{36} fatty acid
448 methyl esters and $C_{36:2}$ fatty acid ethyl ester elute before the $C_{37:2}$ and $C_{37:3}$ Me ketones (3.5 -
449 4.5 min; Fig. 3a). Because of the co-elution of all C_{37} LCAs, the $^{13}C_2$ isotopic peak of the $C_{37:3}$
450 LCA (i.e. the second isotope peak which has the same *m/z* value as the $C_{37:2}$ LCA) contributes
451 to the monoisotopic peak of the $C_{37:2}$ LCA, and thus the peak area of the $C_{37:2}$ LCA requires
452 correction in order to quantify the $U^{K'}_{37}$. The fractional abundance of this $^{13}C_2$ isotopic peak is
453 7.79% of the monoisotopomer (theoretically determined). Consequently, when quantifying co-
454 eluting C_{37} LCAs or calculating the $U^{K'}_{37}$ index on single quadrupole UHPLC-MS using SIM
455 or UHPLC-HRMS, the peak area of the $C_{37:2}$ LCA has to be corrected by subtracting $0.0779 \times$
456 $\text{area}_{C_{37:3}}$ from the peak area of the $C_{37:2}$ LCA. In this culture, we did not detect the $C_{37:4}$ LCA.
457 However, when present (normally produced under low temperatures or in freshwater
458 environments [34]), its $^{13}C_2$ peak would in turn contribute to the area of the $C_{37:3}$ LCA. This
459 contribution would be the same, and hence, also the correction.

460

461 *3.3.2 LOD and LOQ*

462 We used a serially diluted *E. huxleyi* alkenone fraction in order to determine the LOD of the
463 $C_{37:2}$ LCA and the LOQ of the $U^{K'}_{37}$ for the different methods. To quantify the amount of $C_{37:2}$
464 LCAs in the *E. huxleyi* alkenone fraction, we added 10-nonadecanone ($C_{19:0}$ ketone) as standard
465 and analyzed the extract by GC-FID assuming equal response factors for the LCAs and 10-
466 nonadecanone. For GC-FID, a LOD of ca. 3 ng $C_{37:2}$ LCA injected on-column was evident (Fig.

8), in agreement with detection limits of 5 to 10 ng previously reported [7]. The LOD for both the UHPLC-MS and UHPLC-HRMS is ca. 1 pg and ca. 2 pg LCA injected on-column, respectively, 3 orders of magnitude lower than for GC-FID. Based on significant deviation of the $U^{K'}_{37}$ values (two-tailed t-test p-value < 0.05) for the lowest amounts injected, as compared to the average $U^{K'}_{37}$ calculated from the higher concentrations (Fig. 8), we define LOQs of the $U^{K'}_{37}$ index of ca. 2 and ca. 20 pg C_{37} LCA injected on-column for UHPLC-MS and UHPLC-HRMS, respectively.

3.3.3 Reproducibility and linearity

The reproducibility of the $U^{K'}_{37}$ (above LOQ) on the single quadrupole UHPLC-MS was ±0.0032 (n = 33) and ±0.0021 (n = 24) on the UHPLC-HRMS which is similar to that obtained for GC-FID (±0.0028; n = 6). The responses (peak area versus amount of $C_{37:2}$ alkenone (pmol) injected on-column) were linear for both methods (Table 3). This contrast the results of chemical ionization MS in a GC/MS method (GC-IC-MS) for quantitation of LCAs which has shown a substantial non-linear response [35]. However, these authors have analyzed higher amounts C_{37} LCAs, i.e., up to ca. 160 ng injected on-column, whereas we have analyzed between ca. 0.4 pg and 4 ng, and Becker et al. [17] between 10 pg and 10 ng.

3.3.4 Comparison of $U^{K'}_{37}$ values

The average $U^{K'}_{37}$ value calculated for the *E. huxleyi* culture fraction on GC-FID is 0.238±0.0028, whereas on single quadrupole UHPLC-MS and UHPLC-HRMS we obtain values of 0.211±0.0032 and 0.267±0.0021, respectively, i.e. there is a significant difference (two-tailed t-test p-value << 0.05) between both UHPLC low (nominal mass) resolution MS and HRMS and GC-FID of 0.026 and 0.029, respectively (Fig. 6). Becker et al. [17] showed

that $U^{K'}_{37}$ values obtained by GC-FID and LC-MS reveal almost a 1:1 relationship, suggesting the suitability of LC-MS for the measurement of the $U^{K'}_{37}$ index. This contrasts, for example, with the findings of Hefter [15], who observed different relative linear responses for the $C_{37:2}$ and $C_{37:3}$ LCAs leading to different $U^{K'}_{37}$ values for a GC-TOF-MS method as compared to GC-FID. However, as for LCDs, standards are required to monitor the relative responses of the $U^{K'}_{37}$ LCAs on LC-MS.

3.4 Multi-proxy versus individual proxy analysis

As pointed out by Becker et al. [17], a major advantage of using LC-MS for determination of organic proxies is the simultaneous analysis, i.e. the TEX_{86}, $U^{K'}_{37}$ and LDI can be determined in a single run. Fig. 9 shows an example of an environmental sample analyzed for LCDs, LCAs and GDGTs on the Orbitrap NP-UHPLC-HRMS. This method results in the elution of the isoprenoid GDGTs and LCDs in the same retention window (between ca. 16 and 30 min). Our results show that for LCDs, the LOD and LOQ for UHPLC-HRMS (with a resolution of typical TOF MS) is similar to the conventional GC-MS SIM method, while for LCAs the LOD and LOQ are more than two orders of magnitude lower as compared to GC-FID. Hence, in this sense UHPLC-HRMS seems highly suitable for the simultaneous analysis of GDGTs, LCAs and LCDs. Additionally, since HRMS operates in full scan mode, it allows for identification of other compounds, in contrast to SIM methods. Although the analysis time (ca. 1.7 h) is similar to those of the other methods, the significantly reduced sample preparation time, i.e. no need for silylation of LCDs, and separation of alkenone and polar (GDGTs and LCDs) fractions, allows a substantial increased sample throughput. However, a UHPLC-HRMS is relatively expensive, and not available in all paleoclimate labs in contrast to GC-FID and GC-MS instruments. Another alternative, UHPLC low (nominal mass) resolution MS, which is an increasingly used instrument in geochemical labs [36], has an LOQ for LCDs that is an order

of magnitude higher as compared to GC-MS, making this method less suitable, as LCDs are often present in trace amounts in environmental samples.

With respect to the UHPLC methods, we chose to use the NP-UHPLC chromatographic method according to Hopmans et al. [23], as the resolution between several critical pairs of GDGTs is highest using this method [23]. However, this two UHPLC silica column method does not result in chromatographic separation of the $C_{37:2}$ and $C_{37:3}$ LCAs and the isomers are only partially separated in mass, requiring an isotope contribution correction. In contrast, the protocol of Becker et al. [22] does result in the chromatographical separation of the C_{37} LCAs, but has lesser separation for several critical pairs of GDGTs [23]. Hence, both protocols can be considered equally suitable for multi-proxy analysis.

Although UHPLC-HRMS seems thus highly suitable for the analysis of the TEX_{86}, $U^{K'}_{37}$ and LDI together, we find small but significant differences between LDI and $U^{K'}_{37}$ values obtained with this method in comparison with traditional methods. Even though Becker et al. [17] showed that the $U^{K'}_{37}$ and LDI indices over temperature ranges gave similar values on LC-MS as compared to the traditional methods (i.e., GC-FID and GC-MS, respectively), absolute responses, and relative responses between compounds can differ substantially per MS. For example, the round-robin study of Schouten et al. [36], in which the GDGT indices were compared between 35 laboratories, showed differences in the TEX_{86}, and especially in the BIT index, a proxy for soil organic matter input based on a ratio of branched GDGTs and crenarchaeol. These offsets are likely due to differences in instrumental characteristics. Therefore, it is highly recommended to use standard mixtures to obtain consistent proxy values. The differences in LDI and $U^{K'}_{37}$ values between LC and GC obtained for our culture fractions are ± 1.87 °C and ± 0.84°C, respectively, when translated to temperature. Although these differences are within the calibration errors of the proxies (2°C and 1.5°C for LDI and $U^{K'}_{37}$, respectively), for consistency with studies of e.g. proxy calibrations from different laboratories

using different methods, it would be desirable that standard mixtures would be available.

4. Conclusions

We have developed and compared different methods to analyze LCDs and LCAs. Firstly, we developed a method for automated silylation using a robot autosampler which substantially reduced sample preparation time. We also developed a triple quadrupole GC-MS/MS method for the detection of LCDs, using MRM transitions, resulting in substantial lowering of background levels, and thus increased reliability of identification. Due to this improved selectivity, this method is potentially convenient for detection of LCDs in environmental matrix-rich samples. The LOQ (ca. 0.3 pg C_{28} 1,13-diol injected on-column) is slightly lower than the original GC-MS SIM method (ca. 0.5 pg). The reproducibility was also slightly better. However, for quantification purposes, authentic standards are needed to quantify the LCDs, posing a limitation. Additionally, we have evaluated the multi-proxy approach, i.e. analysis of multiple proxies with a single method as introduced by Becker et al. [17], using the NP-UHPLC method of Hopmans et al. [23] combined with Orbitrap HRMS and single quadrupole UHPLC-MS. The HRMS revealed for LCDs a similar sensitivity as GC-MS (LOQ ca. 1.5 pg), and the best reproducibility. In contrast, the LOQ of the low (nominal mass) resolution MS was more than one order of magnitude higher (ca. 15 pg) as compared to the traditional GC-MS method, and therefore less suitable for the analysis of LCDs. The LOQ of the LCAs used for determination of the $U^{K'}_{37}$ index was also in the pg range for both UHPLC-HRMS and UHPLC-MS, which is a substantial improvement as compared to the detection limit of 5 – 10 ng on GC-FID. Although UHPLC-HRMS is an excellent method for multi-proxy analysis, standard mixtures are recommended to enable quantification and monitor the absolute response of the LCAs and LCDs.

565

566 **Acknowledgements**

567 This research has been funded by the European Research Council (ERC) under the European
568 Union's Seventh Framework Program (FP7/2007-2013) ERC grant agreement [339206] to S.S.
569 S.S. and J.S.S.D. receive financial support from the Netherlands Earth System Science Centre
570 (NESSC). We thank Dr. David Chivall for growing the *Emiliani huxleyi* culture used in the
571 experiments.

572

573 **References**

574 [1] S. Schouten, E.C. Hopmans, E. Schefuss, J.S.S. Damste, Distributional variations in marine
575 crenarchaeotal membrane lipids: a new tool for reconstructing ancient sea water temperatures?,
576 Earth Planet. Sci. Lett., 204 (2002) 265-274.

577 [2] S.C. Brassell, G. Eglinton, I.T. Marlowe, U. Pflaumann, M. Sarnthein, Molecular
578 stratigraphy – A new tool for climatic assessment, Nature, 320 (1986) 129-133.

579 [3] S.W. Rampen, V. Willmott, J.H. Kim, E. Uliana, G. Mollenhauer, E. Schefuss, J.S.S.
580 Damste, S. Schouten, Long chain 1,13-and 1,15-diols as a potential proxy for
581 palaeotemperature reconstruction, Geochim. Cosmochim. Acta, 84 (2012) 204-216.

582 [4] G.J.M. Versteegh, H.J. Bosch, J.W. de Leeuw, Potential palaeoenvironmental information
583 of C_{24} to C_{36} mid-chain diols, keto-ols and mid-chain hydroxy fatty acids; a critical review, Org.
584 Geochem., 27 (1997) 1-13.

585 [5] J.K. Volkman, S.M. Barrett, G.A. Dunstan, S.W. Jeffrey, C_{30}-C_{32} alkyl diols and unsaturated
586 alcohols in microalgae of the class Eustigmatophyceae, Org. Geochem., 18 (1992) 131-138.

587 [6] T.D. Herbert, 6.15 - Alkenone Paleotemperature Determinations A2 - Turekian, Heinrich
588 D. HollandKarl K, in: Treatise on Geochemistry, Pergamon, Oxford, 2003, pp. 391-432.

589 [7] J. Villanueva, J.O. Grimalt, Gas chromatographic tuning of the $U^{K'}_{37}$ paleothermometer,
590 Anal. Chem., 69 (1997) 3329-3332.

591 [8] J.O. Grimalt, E. Calvo, C. Pelejero, Sea surface paleotemperature errors in $U^{K'}_{37}$ estimation
592 due to alkenone measurements near the limit of detection, Paleoceanography, 16 (2001) 226-
593 232.

594 [9] J. Villanueva, C. Pelejero, J.O. Grimalt, Clean-up procedures for the unbiased estimation of
595 C_{37} alkenone sea surface temperatures and terrigenous *n*-alkane inputs in paleoceanography, J.
596 Chromatogr. A, 757 (1997) 145-151.

597 [10] W.M. Longo, J.T. Dillon, R. Tarozo, J.M. Salacup, Y.S. Huang, Unprecedented separation
598 of long chain alkenones from gas chromatography with a poly(trifluoropropylmethylsiloxane)
599 stationary phase, Org. Geochem., 65 (2013) 94-102.

600 [11] L. Xu, C.M. Reddy, J.W. Farrington, G.S. Frysinger, R.B. Gaines, C.G. Johnson, R.K.
601 Nelson, T.I. Eglinton, Identification of a novel alkenone in Black Sea sediments, Org.
602 Geochem., 32 (2001) 633-645.

603 [12] A. Rosell-melé, J.F. Carter, A.T. Parry, G. Eglinton, Determination of the $U^{K'}_{37}$ index in
604 geological samples, Anal. Chem., 67 (1995) 1283-1289.

605 [13] R. Chaler, J.O. Grimalt, C. Pelejero, E. Calvo, Sensitivity effects in $U^{K'}_{37}$ paleotemperature
606 estimation by chemical ionization mass spectrometry, Anal. Chem., 72 (2000) 5892-5897.

607 [14] J.F. Rontani, F.G. Prahl, J.K. Volkman, Characterization of unusual alkenones and alkyl
608 alkenoates by electron ionization gas chromatography/mass spectrometry, Rapid Commun.
609 Mass Spectrom., 20 (2006) 583-588.

610 [15] J. Hefter, Analysis of alkenone unsaturation indices with fast gas chromatography/time-
611 of-flight mass spectrometry, Anal. Chem., 80 (2008) 2161-2170.

612 [16] V.F. Schwab, J.P. Sachs, The measurement of D/H ratio in alkenones and their isotopic
613 heterogeneity, Org. Geochem., 40 (2009) 111-118.

614 [17] K.W. Becker, J.S. Lipp, G.J.M. Versteegh, L. Wormer, K.U. Hinrichs, Rapid and
615 simultaneous analysis of three molecular sea surface temperature proxies and application to
616 sediments from the Sea of Marmara, Org. Geochem., 85 (2015) 42-53.

617 [18] E.C. Hopmans, S. Schouten, R.D. Pancost, M.T.J. van der Meer, J.S.S. Damste, Analysis
618 of intact tetraether lipids in archaeal cell material and sediments by high performance liquid
619 chromatography/atmospheric pressure chemical ionization mass spectrometry, Rapid
620 Commun. Mass Spectrom., 14 (2000) 585-589.

621 [19] M. Escala, S. Fietz, G. Rueda, A. Rosell-Mele, Analytical Considerations for the Use of
622 the Paleothermometer Tetraether Index(86) and the Branched vs Isoprenoid Tetraether Index
623 Regarding the Choice of Cleanup and Instrumental Conditions, Anal. Chem., 81 (2009) 2701-
624 2707.

625 [20] S. Schouten, A. Forster, F.E. Panoto, J.S.S. Damste, Towards calibration of the TEX_{86}
626 palaeothermometer for tropical sea surface temperatures in ancient greenhouse worlds, Org.
627 Geochem., 38 (2007) 1537-1546.

628 [21] C. Zhu, J.S. Lipp, L. Wormer, K.W. Becker, J. Schroder, K.U. Hinrichs, Comprehensive
629 glycerol ether lipid fingerprints through a novel reversed phase liquid chromatography-mass
630 spectrometry protocol, Org. Geochem., 65 (2013) 53-62.

631 [22] K.W. Becker, J.S. Lipp, C. Zhu, X.L. Liu, K.U. Hinrichs, An improved method for the
632 analysis of archaeal and bacterial ether core lipids, Org. Geochem., 61 (2013) 34-44.

633 [23] E.C. Hopmans, S. Schouten, J.S.S. Damste, The effect of improved chromatography on
634 GDGT-based palaeoproxies, Org. Geochem., 93 (2016) 1-6.

635 [24] J.W. de Leeuw, W. Irene, C. Rijpstra, P.A. Schenck, J.K. Volkman, Free, esterified and
636 residual bound sterols in Black-Sea Unit-I, Geochim. Cosmochim. Acta, 47 (1983) 455-465.

637 [25] M. Rodrigo-Gámiz, S.W. Rampen, H. de Haas, M. Baas, S. Schouten, J.S.S. Damste,
638 Constraints on the applicability of the organic temperature proxies $U^{K'}_{37}$, TEX_{86} and LDI in the
639 subpolar region around Iceland, Biogeosciences, 12 (2015) 6573-6590.

640 [26] C. Zell, J.H. Kim, M23]. Balsinha, D. Dorhout, C. Fernandes, M. Baas, J.S.S. Damste,
641 Transport of branched tetraether lipids from the Tagus River basin to the coastal ocean of the
642 Portuguese margin: consequences for the interpretation of the MBT'/CBT paleothermometer,
643 Biogeosciences, 11 (2014) 5637-5655.

644 [27] C. Zell, J.H. Kim, D. Dorhout, M. Baas, J.S.S. Damste, Sources and distributions of
645 branched tetraether lipids and crenarchaeol along the Portuguese continental margin:
646 Implications for the BIT index, Continental Shelf Research, 96 (2015) 34-44.

647 [28] M. Rodrigo-Gámiz, F. Martinez-Ruiz, S.W. Rampen, S. Schouten, J.S.S. Damste, Sea
648 surface temperature variations in the western Mediterranean Sea over the last 20 kyr: A dual-
649 organic proxy ($U^{K'}_{37}$ and LDI) approach, Paleoceanography, 29 (2014) 87-98.

650 [29] D. Chivall, D. M'Boule, D. Sinke-Schoen, J.S.S. Damste, S. Schouten, M.T.J. van der
651 Meer, Impact of salinity and growth phase on alkenone distributions in coastal haptophytes,
652 Org. Geochem., 67 (2014) 31-34.

653 [30] F.G. Prahl, S.G. Wakeham, Calibration of unsaturation patterns in long-chain ketone
654 compositions for paleotemperature assessment, Nature, 330 (1987) 367-369.

655 [31] P.J. Muller, G. Kirst, G. Ruhland, I. von Storch, A. Rosell-Mele, Calibration of the
656 alkenone paleotemperature index $U^{K'}_{37}$ based on core-tops from the eastern South Atlantic and
657 the global ocean (60 degrees N-60 degrees S), Geochim. Cosmochim. Acta, 62 (1998) 1757-
658 1772.

659 [32] M.W. de Bar, D.J.C. Dorhout, E.C. Hopmans, S.W. Rampen, J.S.S. Damste, S. Schouten,
660 Constraints on the application of long chain diol proxies in the Iberian Atlantic margin, Org.
661 Geochem., 101 (2016) 184-195.

662 [33] A. Rosell-Melé, E. Bard, K.C. Emeis, J.O. Grimalt, P. Muller, R. Schneider, I.
663 Bouloubassi, B. Epstein, K. Fahl, A. Fluegge, K. Freeman, M. Goni, U. Guntner, D. Hartz, S.
664 Hellebust, T. Herbert, M. Ikehara, R. Ishiwatari, K. Kawamura, F. Kenig, J.W. de Leeuw, S.
665 Lehman, L. Mejanelle, N. Ohkouchi, R.D. Pancost, C. Pelejero, F. Prahl, J. Quinn, J.F. Rontani,
666 F. Rostek, J. Rullkotter, J. Sachs, T. Blanz, K. Sawada, D. Schulz-Bull, E. Sikes, C. Sonzogni,
667 Y. Ternois, G. Versteegh, J.K. Volkman, S. Wakeham, Precision of the current methods to
668 measure the alkenone proxy $U^{K'}_{37}$ and absolute alkenone abundance in sediments: Results of
669 an interlaboratory comparison study, Geochem. Geophys. Geosyst., 2 (2001).

670 [34] F.G. Prahl, L.A. Muehlhausen, D.L. Zahnle, Further evaluation of long-chain alkenones
671 as indicators of paleoceanographic conditions, Geochim. Cosmochim. Acta, 52 (1988) 2303-
672 2310.

673 [35] R. Chaler, J. Villanueva, J.O. Grimalt, Non-linear effects in the determination of
674 paleotemperature U-37(k ') alkenone ratios by chemical ionization mass spectrometry, J.
675 Chromatogr. A, 1012 (2003) 87-93.

676 [36] S. Schouten, E.C. Hopmans, A. Rosell-Melé, A. Pearson, P. Adam, T. Bauersachs, E. Bard,
677 S.M. Bernasconi, T.S. Bianchi, J.J. Brocks, L.T. Carlson, I.S. Castaneda, S. Derenne, A.D.

678 Selver, K. Dutta, T. Eglinton, C. Fosse, V. Galy, K. Grice, K.U. Hinrichs, Y.S. Huang, A.
679 Huguet, C. Huguet, S. Hurley, A. Ingalls, G. Jia, B. Keely, C. Knappy, M. Kondo, S. Krishnan,
680 S. Lincoln, J. Lipp, K. Mangelsdorf, A. Martinez-Garcia, G. Menot, A. Mets, G. Mollenhauer,
681 N. Ohkouchi, J. Ossebaar, M. Pagani, R.D. Pancost, E.J. Pearson, F. Peterse, G.J. Reichart, P.
682 Schaeffer, G. Schmitt, L. Schwark, S.R. Shah, R.W. Smith, R.H. Smittenberg, R.E. Summons,
683 Y. Takano, H.M. Talbot, K.W.R. Taylor, R. Tarozo, M. Uchida, B.E. van Dongen, B.A.S. Van
684 Mooy, J.X. Wang, C. Warren, J.W.H. Weijers, J.P. Werne, M. Woltering, S.C. Xie, M.
685 Yamamoto, H. Yang, C.L. Zhang, Y.G. Zhang, M.X. Zhao, J.S.S. Damste, An interlaboratory
686 study of TEX_{86} and BIT analysis of sediments, extracts, and standard mixtures, Geochem.
687 Geophys. Geosyst., 14 (2013) 5263-5285.

688

689

690 **Figure 1.** Structures of some long chain alkenones, isoprenoid GDGTs and long chain diols.

691 **Figure 2.** Panel 3a shows the mass spectrum (MS^1) of the silylated C_{30} 1,15-diol and the typical
692 fragmentations adjacent to the OTMSi group are indicated, resulting in the characteristic
693 product ions with *m/z* 313 and 387. The MS^2 product ions scans of the characteristic mass
694 fragments with *m/z* 313 (quantifier ion) and 387 (qualifier ion) are shown in panel 3b and 3c,
695 respectively. The product ions selected in the second stage of mass filtering (*m/z* 103 and 109)
696 are in bold.

697 **Figure 3.** Partial total ion currents of the *E. huxleyi* (panel a) and *N. oculata* fractions (panel b)
698 analyzed by UHPLC-HRMS (*m/z* 400 – 1450). Me = methyl; Et = ethyl; FAME = fatty acid
699 methyl ester; FAEE = fatty acid ethyl ester.

700 **Figure 4.** LDI values versus the amounts of C_{28} 1,13-diol injected on-column for different
701 methods (GC-MS/MS using MRM, GC-MS using SIM for two different MS detectors (dark
702 green = 7000 C GC/MS Triple Quad and light green = Agilent 5977A MS), Orbitrap UHPLC-
703 HRMS and UHPLC-MS using SIM. LCDs were extracted from a *Nannochloropsis oculata*
704 culture. The error bars reflect ± 1σ standard deviation from triplicate measurements; when not
705 visible, the error bars are smaller than the symbol size.

706 **Figure 5.** SIM and MRM chromatograms (left and right) of a sediment sample deriving from
707 the Portuguese margin [27,32]. As identification in MRM mode is based upon the presence of
708 two target ions, selectivity is improved.

709 **Figure 6.** Average LDI and $U^{K'}_{37}$ values for the *N. oculata* and *E. huxleyi* culture, respectively,
710 obtained using the different methods. The black error bars reflect reproducibility; the red error
711 bars represent the calibration errors (2 ^{0}C for LDI; 1,5 ^{0}C for $U^{K'}_{37}$). All proxy values are
712 significantly different from each other, as well as from the values obtained by the traditional

methods (GC-MS for LDI, GC FID for $U^{K'}_{37}$; * = *p*-value < 0.005; ** = difference is larger than calibration error). S.q. = single quadrupole; t.q. = triple quadrupole.

Figure 7. Cross-plot of LDI values determined by GC-MS using SIM (Agilent 5977A mass spectrometer) and GC-MS/MS using MRM (7000 C GC/MS Triple Quad). The orange dashed line represents the 1:1 line.

Figure 8. $U^{K'}_{37}$ values versus the amounts of $C_{37:2}$ alkenone injected on-column for different methods (UHPLC-HRMS, UHPLC-MS and GC-FID). LCAs were extracted from an *Emiliana huxleyi* culture. The dotted lines represent the average $U^{K'}_{37}$ values within the linear response ranges. The error bars reflect ± 1σ standard deviation from triplicate measurements for UHPLC and duplicates for GC; when not visible, the error bars are smaller than the symbol size.

Figure 9. The upper panel shows the total ion current (TIC) of a sediment sample deriving from the Alboran Sea [28] analyzed on the Orbitrap UHPLC-HRMS. The lower three panels show partial extracted ion chromatograms (0 - 40 min) of long chain alkenones, long chain diols and isoprenoid GDGTs (from top to bottom).

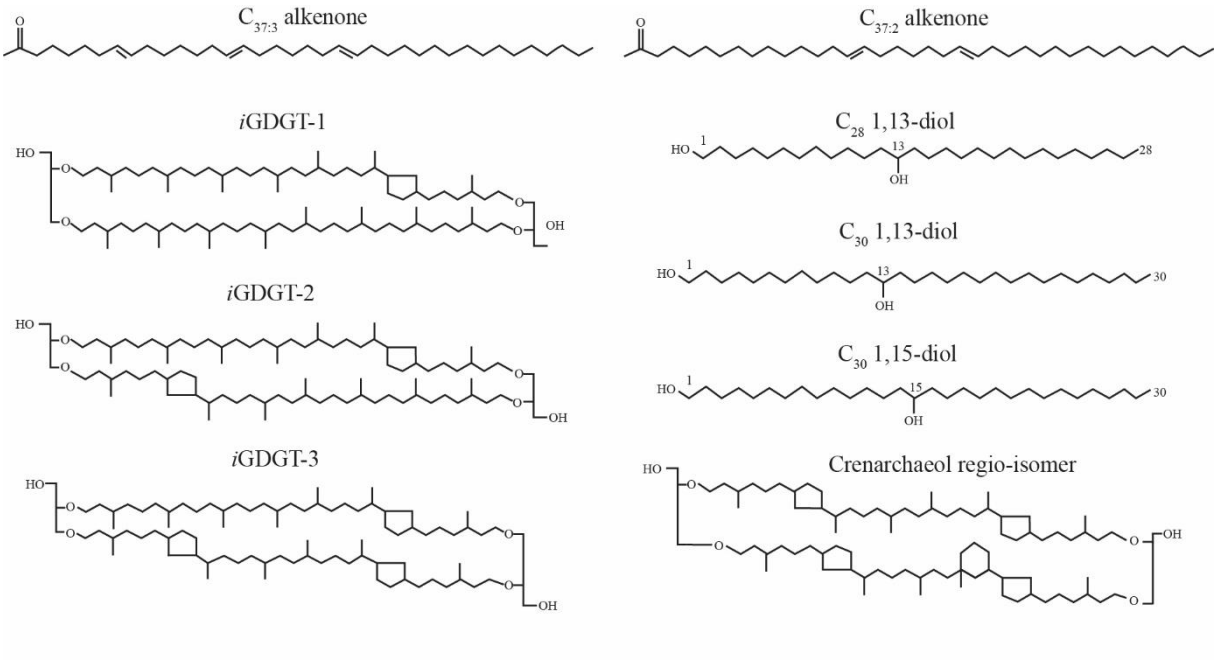

729

730 **Fig. 1**

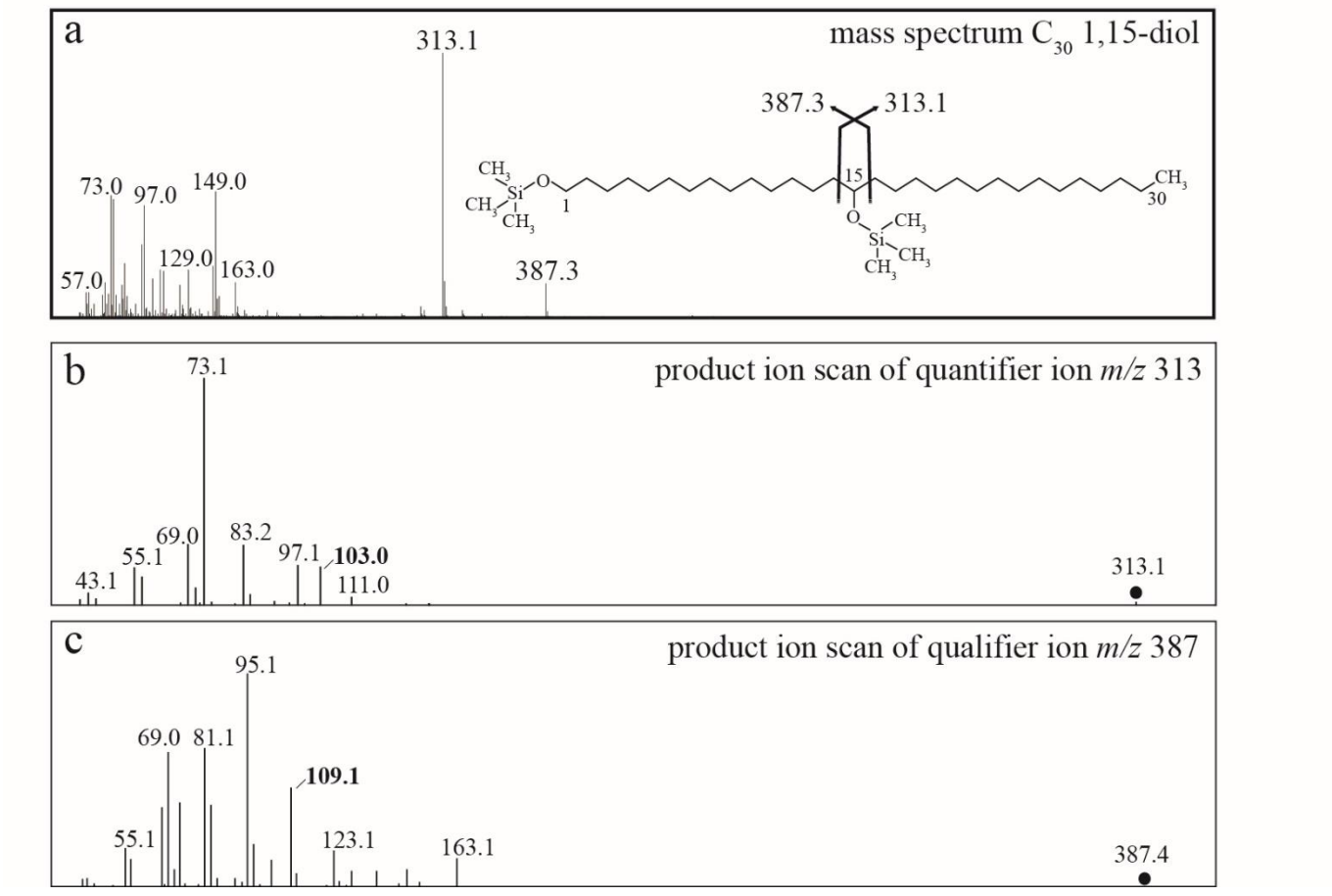

731

732 **Fig. 2**

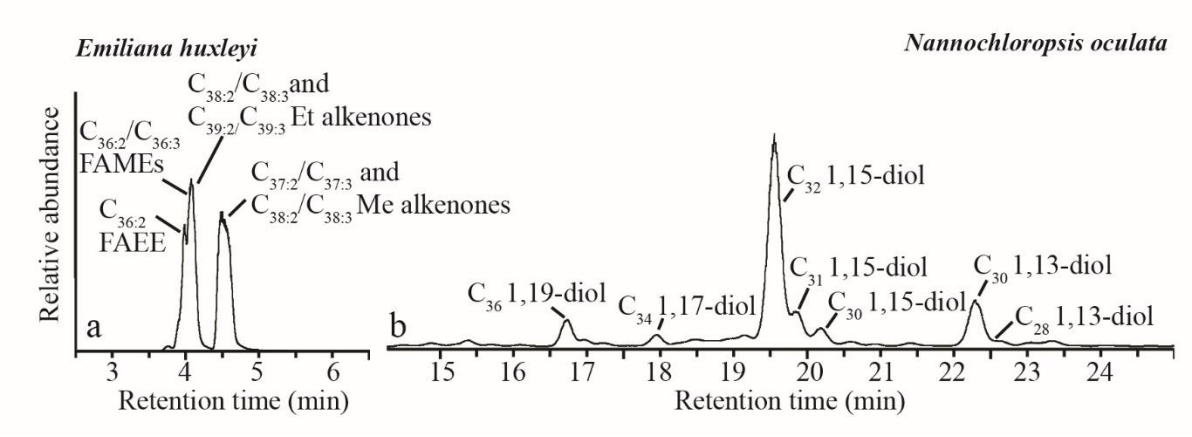

733

734 **Fig. 3**

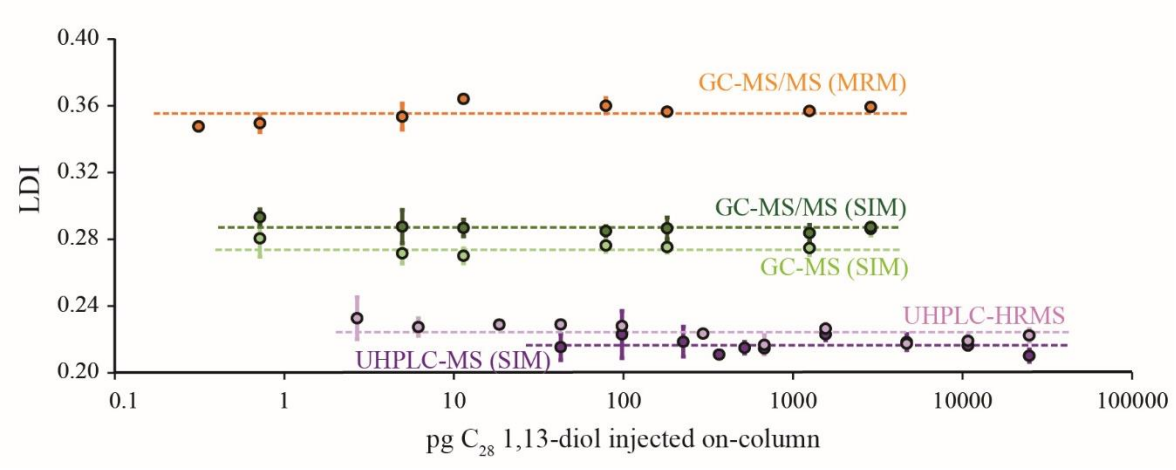

735

736 **Fig. 4**

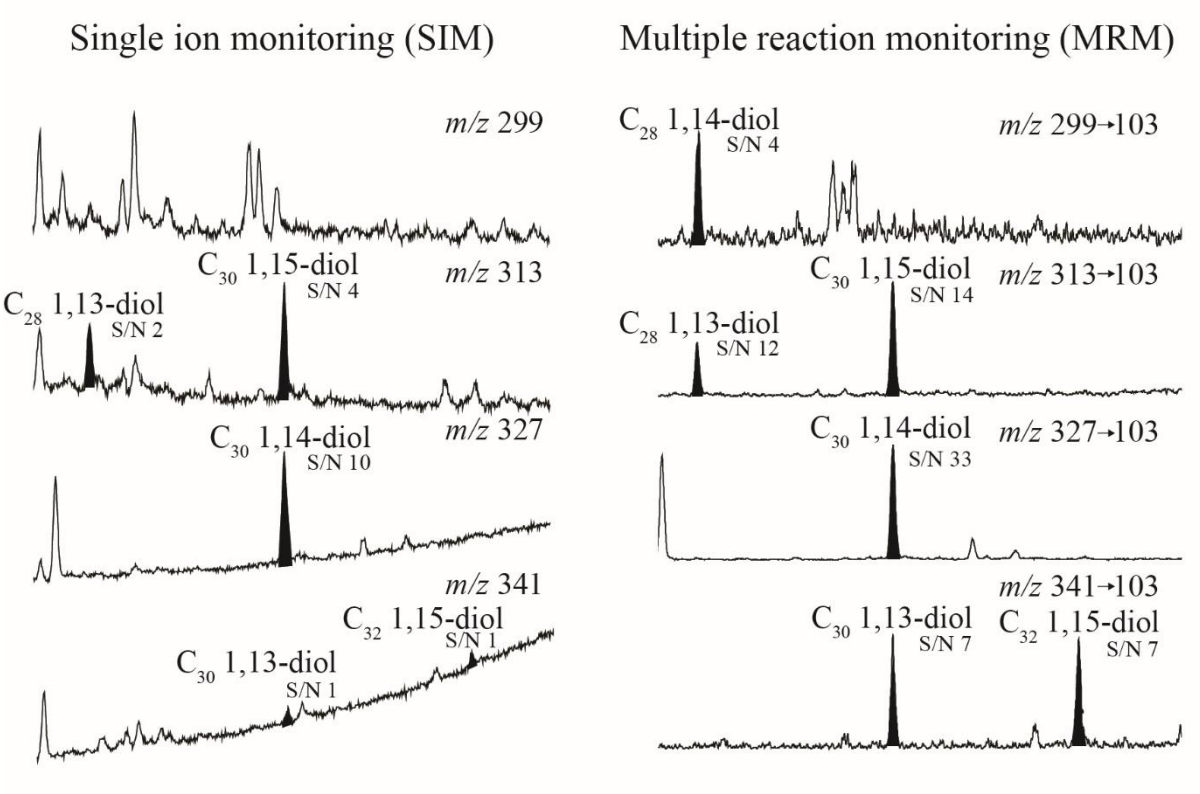

737

738 **Fig. 5**

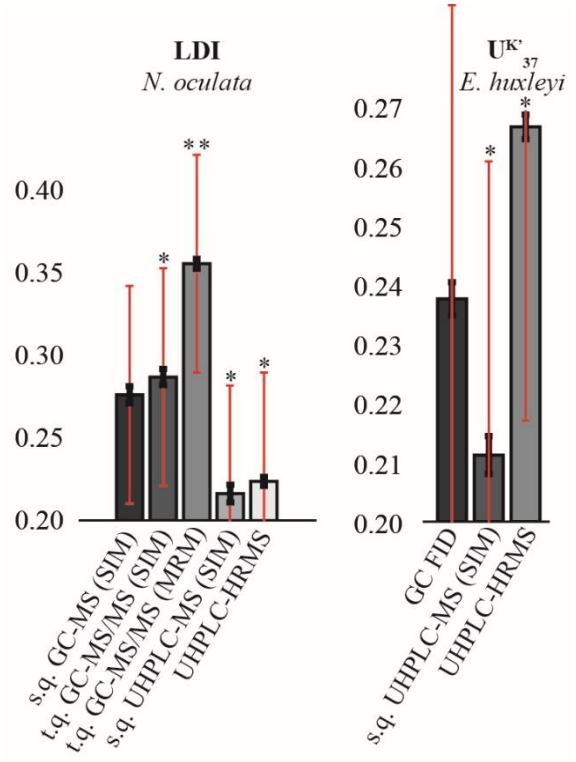

739

740 **Fig. 6**

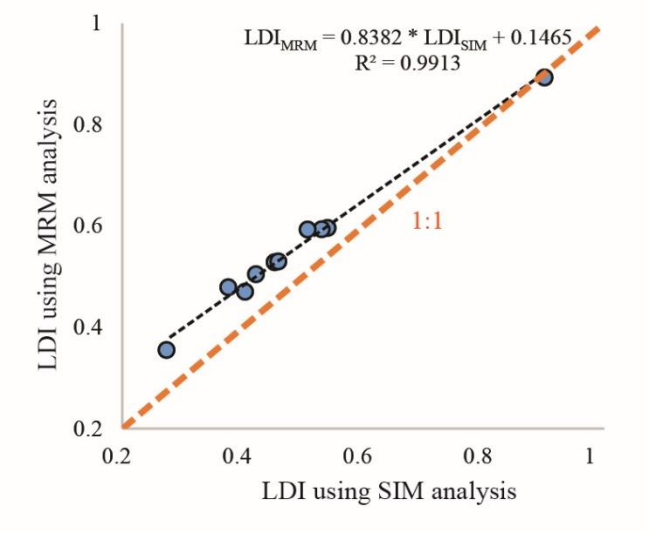

741

742 **Fig. 7**

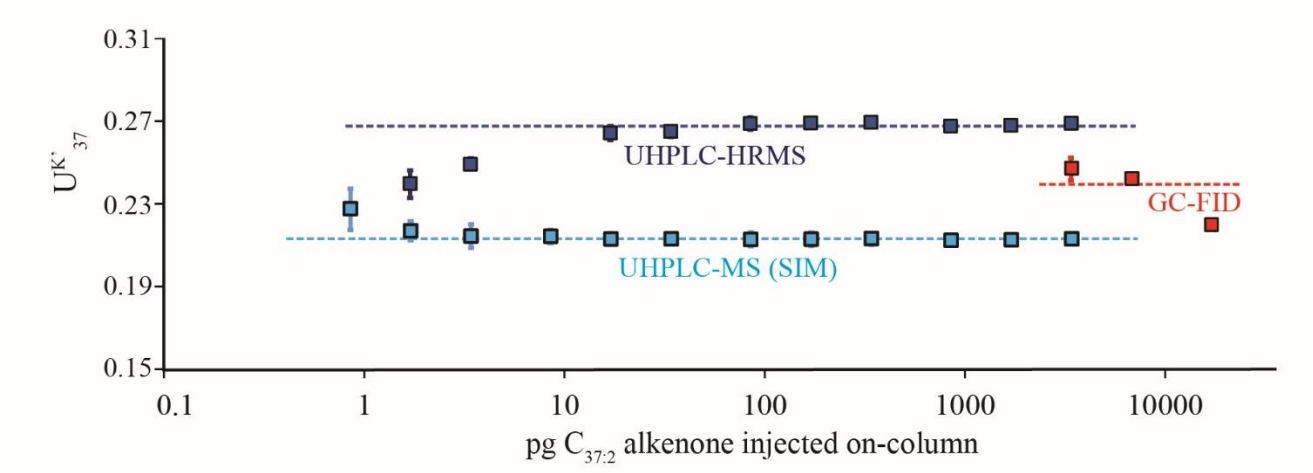

743

744 **Fig. 8**

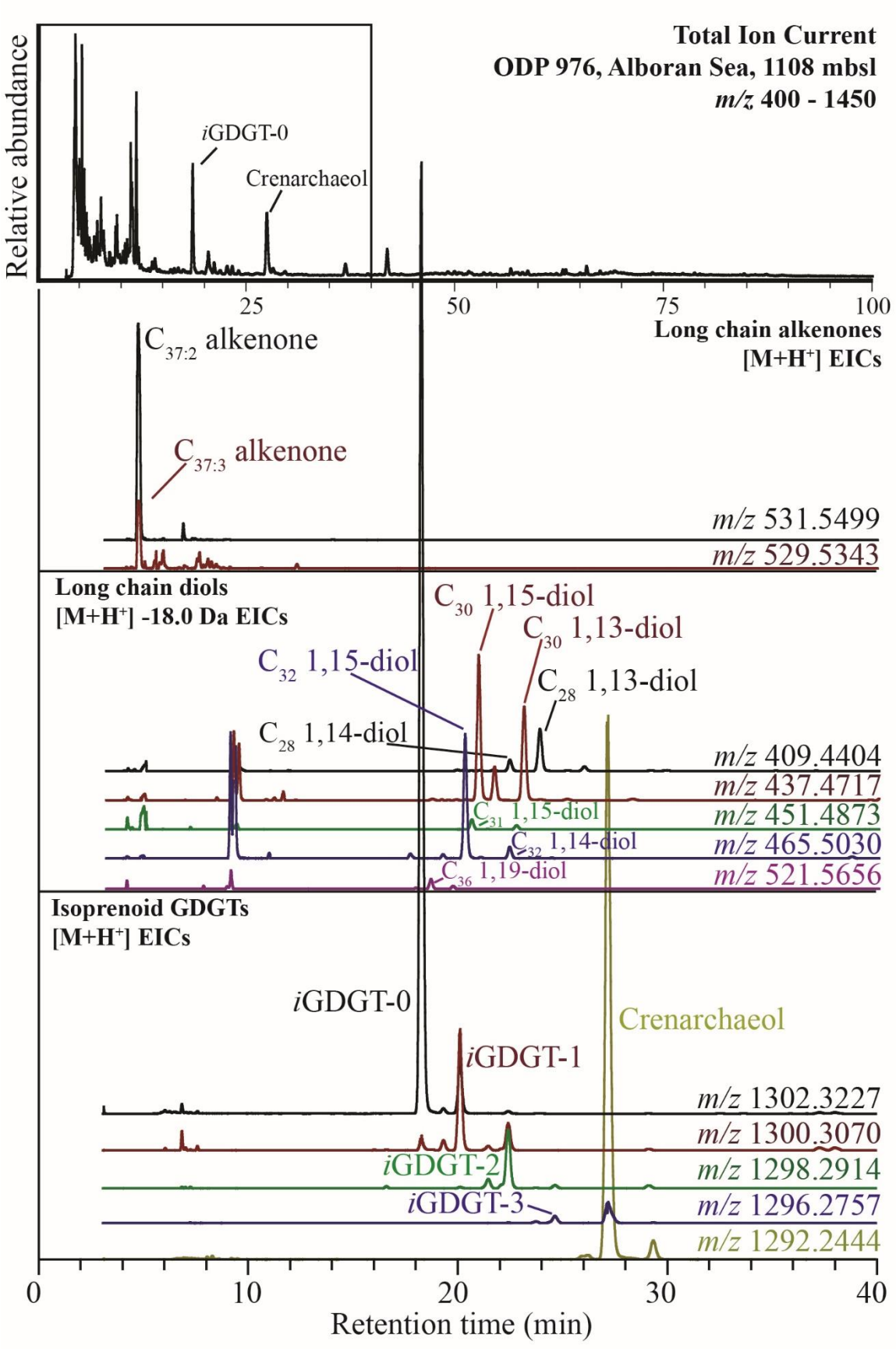
Total Ion Current
ODP 976, Alboran Sea, 1108 mbsl
m/z 400 - 1450
Relative abundance
iGDGT-0
Crenarchaeol
25
50
75
100
Long chain alkenones
[M+H+] EICs
C37:2 alkenone
C37:3 alkenone
m/z 531.5499
m/z 529.5343
Long chain diols
[M+H+] -18.0 Da EICs
C30 1,15-diol
C30 1,13-diol
C32 1,15-diol
C28 1,13-diol
C28 1,14-diol
m/z 409.4404
m/z 437.4717
C31 1,15-diol
m/z 451.4873
C32 1,14-diol
m/z 465.5030
C36 1,19-diol
m/z 521.5656
Isoprenoid GDGTs
[M+H+] EICs
iGDGT-0
Crenarchaeol
iGDGT-1
m/z 1302.3227
m/z 1300.3070
iGDGT-2
m/z 1298.2914
iGDGT-3
m/z 1296.2757
m/z 1292.2444
0
10
20
30
40
Retention time (min)

745

746 **Fig. 9**